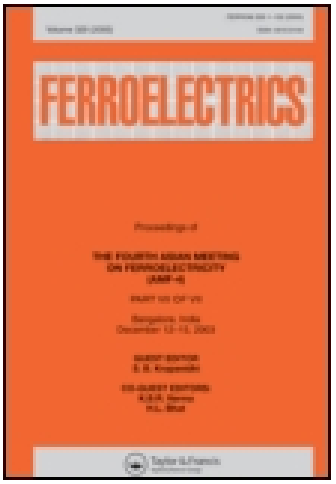

Ferroelectrics
Publication details, including instructions for authors and subscription information:
http://www.tandfonline.com/loi/gfer20

# Novel Time-Domain Circuit Modelling of $\chi^{(2)}$ Nonlinear Process in Periodic Optical Waveguide

Alessandro Massaro [a], Vittoriana Tasco [a], Maria Teresa Todaro [a], Roberto Cingolani [a], Massimo De Vittorio [a] & Adriana Passaseo [a]
[a] National Nanotechnology Laboratory of CNR-INFM, Distretto Tecnologico-ISUFI, Università del Salento, Via Arnesano, 73100, Lecce, Italy
Published online: 20 Sep 2010.

To cite this article: Alessandro Massaro, Vittoriana Tasco, Maria Teresa Todaro, Roberto Cingolani, Massimo De Vittorio & Adriana Passaseo (2009) Novel Time-Domain Circuit Modelling of $\chi^{(2)}$ Nonlinear Process in Periodic Optical Waveguide, Ferroelectrics, 390:1, 62-70, DOI: 10.1080/00150190902993978

To link to this article: http://dx.doi.org/10.1080/00150190902993978

*Ferroelectrics*, 390:62–70, 2009

ISSN: 0015-0193 print / 1563-5112 online
DOI: 10.1080/00150190902993978

Taylor & Francis
Taylor & Francis Group

# Novel Time-Domain Circuit Modelling of $\chi^{(2)}$ Nonlinear Process in Periodic Optical Waveguide

ALESSANDRO MASSARO,* VITTORIANA TASCO, MARIA TERESA TODARO, ROBERTO CINGOLANI, MASSIMO DE VITTORIO, AND ADRIANA PASSASEO**

National Nanotechnology Laboratory of CNR-INFM, Distretto Tecnologico-ISUFI, Università del Salento, Via Arnesano, 73100 Lecce, Italy

*In this work we present a new time domain modelling approach of $\chi^{(2)}$ nonlinear processes in periodic slab waveguides and cavities. This method exploits the Hertzian Potential Modelling (HPM) to design discontinuous dielectric interfaces. It is based on a circuital approach which considers the time-domain nonlinear wave propagation in transmission lines coupled with voltage and current generators. These generators are placed directly on the interface nodes thus optimizing the numerical error of the temporal second derivatives at the dielectric boundaries, and providing an accurate characterization of the nonlinear processes in integrated optics.*

**Keywords** Time domain modelling; nonlinear optical circuits



## 1. Introduction

The modelling of nonlinear devices by a time domain simulator containing second-order nonlinearities is performed. The simulation algorithm is based on nonlinear wave equations associated to the circuital approach which considers the time-domain nonlinear wave propagating in transmission lines. The transmission lines represent the propagating modes of a non linear optical waveguide. Each propagating mode is solution of the scalar Helmholtz wave equation [1–5] and is associated to a transmission line with a characteristic impedance which depends on the modal effective refractive index [1]. This analogy allows to model a nonlinear optical waveguide as a set of transmission line circuits which take into account the dielectric interfaces along the propagating direction as voltage and current generators. The modelling of discontinuous optical waveguides by generators provides less computational time consuming with good convergent solutions [5]. In fact the generators are placed directly on the interface nodes thus optimizing the numerical error of the temporal second derivatives at the dielectric boundary condition. In this way it is also possible to discretise and solve complex dielectric thin multilayer structures with spatial cells of the same order of the dielectric thicknesses [5]. Especially the numerical approximation (voltage and current generators) combined with the analytical approximation (effective dielectric constant (EDC)

Received July 29, 2008; in final form September 8, 2008.
*Corresponding author. E-mail: alessandro.massaro@unile.it
**Permanent address: IMM-CNR Sezione Lecce, University Campus, Lecce Monteroni 73100, Italy.

method) allows to model a two-dimensional (2D) or a three-dimensional (3D) nonlinear waveguide with a good numerical convergent solution making the proposed formulation more attractive than the full-wave solution, especially in three-dimensional complex optical devices with typical sizes is sought. By using the Helmholtz equations to represent the propagating fields in a nonlinear medium, the nonlinear field solution is reduced to an equivalent scalar problem. For a 2-D second harmonic generation (SHG) problem, for example, the proposed time-domain algorithm solves harmonic field. The same problem, solved by the conventional finite difference time domain (FDTD) algorithm for three correlated field components requires a central processing unit (CPU) time 50 times higher. In a 3D case the proposed algorithm solves again two scalar equations instead of six, and subsequently all the electromagnetic (EM) field components are obtained by the two scalar potentials as in Hertzian potential formulation (HPM) [4, 5]. In the time-domain characterization of nonlinear optical structures EM detailed analysis is not necessary even though an accurate numerical solution in proximity of dielectric interfaces is required. In this work, by means of this circuit modelling approach, we model and analyze the $\chi^{(2)}$ non linear processes of asymmetrical slab waveguide with nonlinear core and dielectric discontinuities. This approach results suitable for the modelling of cavity structures. The scalar potentials used allow to evaluate the fundamental and the second harmonic (SH) fields as two modes which propagate independently in two transmission lines with generators corresponding to the dielectric interfaces (see Fig. 1a), b)). The same circuital model is applied to a nonlinear cavity. In particular the nonlinear cavity is modelled by considering a source signal inside the cavity of length L, and current/voltages generators in proximity of the dielectric interfaces. Moreover in the spontaneous parametric down conversion process, a 2D time domain circuit model describes the upward and the downward photon pair characterization.

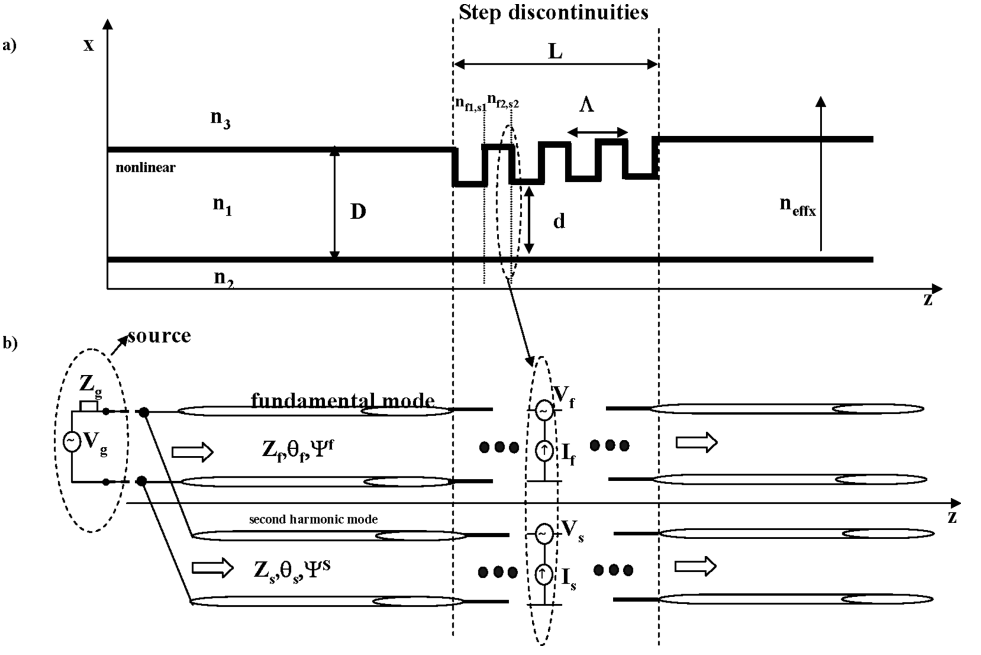


**Figure 1.** a) Asymmetrical slab waveguide with nonlinear core; b) related transmission line model with generators for a second harmonic process. The effective refractive indices $n_{f,s}$ refer to the effective fundamental refractive index $n_f$ and to the effective second harmonic refractive index $n_s$. $Z_g$ is the source impedance and represents a not ideal source.

## 2. Circuital Time-Domain Modellling of SHG Processes

The formulation of the fundamental and second-harmonic fields starts with the Helmholtz wave equation for an homogeneous non-dissipative medium:

$$\nabla^2 \Psi_{e,h}(x, y, z, t) - \mu \varepsilon_{eff} \frac{\partial^2 \Psi_{e,h}(x, y, z, t)}{\partial t^2} = 0 \tag{1}$$

where $\psi_e$ and $\psi_h$ represent two guided modes of the asymmetrical waveguide shown in Fig. 1 (a), and $\varepsilon_{eff}$ is the effective permittivity index evaluated by the effective dielectric constant (EDC) approach method [5]. Each mode propagates in the optical waveguide as a signal which travels in a transmission line (see Fig. 1 (b)) characterized by a characteristic impedance given by

$$Z_{e,h} = \frac{1}{\sqrt{\varepsilon_{eff_{e,h}}}} \sqrt{\frac{\mu_0}{\varepsilon_0}} \tag{2}$$

It is known that the scalar wave equation may lead to inconsistencies because, in inhomogeneous regions such as step discontinuities shown in Fig. 1 (a), it is, in general, not equivalent to Maxwell's equations. Electromagnetic scattering problems, including free space, involve the calculation of the fields produced in the presence of geometrical discontinuities by arbitrary currents and voltages [4]. Such discontinuities may be replaced by equivalent generators [4, 5], (see Fig. 1 (b)), giving an accurate solution of the EM field for structures with high dielectric contrast. In fact the scalar wave equation (1) for a non-dissipative medium can be rewritten as

$$\nabla^2 \Psi_{e,h}(x, y, z, t) - \mu \varepsilon_{eff} \frac{\partial^2 \Psi_{e,h}(x, y, z, t)}{\partial t^2} - \mu \frac{\partial^2 P^{e,h}_{pert}(x, y, z, t)}{\partial t^2} = 0 \tag{3}$$

where

$$P^{e,h}_{pert}(x, y, z, t) = \Delta\varepsilon(x, y, z, t) \Psi_{e,h}(x, y, z, t) \tag{4}$$

represents the dielectric polarization and in a 1D case [4]

$$\Delta\varepsilon = \varepsilon_{i+1} - \varepsilon_i \quad i = z \text{ longitudinal position} \tag{5}$$

Equation (3) gives the effect of the generators $V_{f,s}$ and $I_{f,s}$ reported in Fig. 1 (b) as variation of coefficients in the finite difference (FD) field discretisation [4]. In particular the wave solution in the homogeneous region (uniform slab region without discontinuities) is in the iterative form [4]

$$\Psi^{n+1}_{e,h}(i) = \Psi^{n}_{e,h}(i+1)\left(\frac{b}{a}\right) + \Psi^{n}_{e,h}(i)\left(\frac{2a-2b}{a}\right) + \Psi^{n-1}_{e,h}(i)(-1) + \Psi^{n}_{e,h}(i-1)\left(\frac{b}{a}\right) \tag{6}$$

and in the nodes between dielectric interfaces of step discontinuities (inhomogeneous region) becomes:

$$\Psi^{n+1}_{e,h}(i) = \Psi^{n}_{e,h}(i+1)\left(\frac{b}{a'}\right) + \Psi^{n}_{e,h}(i)\left(\frac{2a'-2b}{a'}\right) + \Psi^{n-1}_{e,h}(i)(-1) + \Psi^{n}_{e,h}(i-1)\left(\frac{b}{a'}\right) \tag{7}$$

with

$$a = \frac{\mu\varepsilon}{(\Delta t)^2}$$
$$a' = a + \frac{\mu\Delta\varepsilon}{(\Delta t)^2} \tag{8}$$
$$b = \frac{1}{(\Delta z)^2}$$

We observe that the equation (3) gives convergent solutions by considering also a non fine spatial discretisation, by decreasing the computational cost [5]. In a nonlinear material the wave equation (1) becomes

$$\nabla^2\Psi_{e,h}(x, y, z, t) - \mu_0\varepsilon_0 n^2\frac{\partial^2\Psi_{e,h}(x, y, z, t)}{\partial t^2} - \mu_0\varepsilon_0\frac{\partial^2 P_{NL}^{e,h}(x, y, z, t)}{\partial t^2} = 0 \tag{9}$$

where $P_{NL}^{e,h}$ is the polarization given by $P_{NL}^{e,h} = \chi^{(2)}\Psi_e\Psi_h$,, $n$ is the material refractive index, and $\chi^{(2)}$ is the dispersionless nonlinear susceptibility. The general field formulation considers three different fields propagating at three different frequencies $\Psi_e(\omega_1)$, $\Psi_h(\omega_2)$, $\Psi_g(\omega_3)$ in material exhibiting an instantaneous second-order nonlinearity

$$\nabla^2\Psi_e = \mu_0\varepsilon_0 n_a^2\frac{\partial^2\Psi_e}{\partial t^2} + \mu_0\varepsilon_0\chi^{(2)}(\omega_1)\frac{\partial^2(\Psi_h\Psi_g)}{\partial t^2} \tag{10}$$

$$\nabla^2\Psi_h = \mu_0\varepsilon_0 n_b^2\frac{\partial^2\Psi_h}{\partial t^2} + \mu_0\varepsilon_0\chi^{(2)}(\omega_2)\frac{\partial^2(\Psi_e\Psi_g)}{\partial t^2} \tag{11}$$

$$\nabla^2\Psi_g = \mu_0\varepsilon_0 n_c^2\frac{\partial^2\Psi_g}{\partial t^2} + \mu_0\varepsilon_0\chi^{(2)}(\omega_3)\frac{\partial^2(\Psi_e\Psi_h)}{\partial t^2} \tag{12}$$

where $n_a$, $n_b$, $n_c$ are the refractive indexes of the wave $\Psi_e(\omega_1)$, $\Psi_h(\omega_2)$, $\Psi_g(\omega_3)$ respectively. Coupled equations (10), (11), and (12) can be rewritten as

$$\nabla^2\Psi_e = \mu_0\varepsilon_0 n_a^2\frac{\partial^2\Psi_e}{\partial t^2} + \mu_0\varepsilon_0\chi^{(2)}(\omega_1)\cdot\left(\Psi_h\frac{\partial^2\Psi_g}{\partial t^2} + \Psi_g\frac{\partial^2\Psi_h}{\partial t^2} + 2\frac{\partial\Psi_h}{\partial t}\frac{\partial\Psi_g}{\partial t}\right) \tag{13}$$

$$\nabla^2\Psi_h = \mu_0\varepsilon_0 n_b^2\frac{\partial^2\Psi_h}{\partial t^2} + \mu_0\varepsilon_0\chi^{(2)}(\omega_2)\cdot\left(\Psi_e\frac{\partial^2\Psi_g}{\partial t^2} + \Psi_g\frac{\partial^2\Psi_e}{\partial t^2} + 2\frac{\partial\Psi_e}{\partial t}\frac{\partial\Psi_g}{\partial t}\right) \tag{14}$$

$$\nabla^2\Psi_g = \mu_0\varepsilon_0 n_c^2\frac{\partial^2\Psi_g}{\partial t^2} + \mu_0\varepsilon_0\chi^{(2)}(\omega_3)\cdot\left(\Psi_e\frac{\partial^2\Psi_h}{\partial t^2} + \Psi_h\frac{\partial^2\Psi_e}{\partial t^2} + 2\frac{\partial\Psi_e}{\partial t}\frac{\partial\Psi_h}{\partial t}\right) \tag{15}$$

field in a SHG process, occurs with $\omega_1 = \omega_2 = \omega$ , $\omega_3 = \omega_1 + \omega_2 = 2\omega$ , $\chi^{(2)} = \chi^{(2)}(\omega_1)/2$ $= \chi^{(2)}(\omega_3)$, We observe that equations (13), (14) and (15) for a generic three-wave-mixing process can refer also to a twin photon generation process. The fundamental and the second harmonic and $\Psi^f = \Psi_e = \Psi_h$ ($n_a = n_b = n_f$). In this case the coupled equations to solve are the following

$$\nabla^2\Psi^f = \mu_0\varepsilon_0 n_f^2\frac{\partial^2\Psi^f}{\partial t^2} + 2\mu_0\varepsilon_0\chi^{(2)}\cdot\left(\Psi^f\frac{\partial^2\Psi^s}{\partial t^2} + \Psi^s\frac{\partial^2\Psi^f}{\partial t^2} + 2\frac{\partial\Psi^f}{\partial t}\frac{\partial\Psi^s}{\partial t}\right) \tag{16}$$

$$\nabla^2\Psi^s = \mu_0\varepsilon_0 n_s^2\frac{\partial^2\Psi^s}{\partial t^2} + 2\mu_0\varepsilon_0\chi^{(2)}\cdot\left(\Psi^f\frac{\partial^2\Psi^f}{\partial t^2} + \frac{\partial\Psi^f}{\partial t}\frac{\partial\Psi^f}{\partial t}\right) \tag{17}$$

We observe from equations (16) and (17) that the fundamental $\Psi^f$ and the second harmonic $\Psi^s$ field are characterized by the refractive indexes $n_f$ and $n_s$ respectively. For the asymmetrical slab shown in Fig. 1 (a), $n_f$ represents the effective refractive index along the x-direction at $\omega_1 = \omega_s$ and $n_s$ represents the effective refractive index at $\omega_3 = \omega_f = 2\omega_s$. In this way it is possible to model the second harmonic generation process by two transmission lines as reported in Fig. 1 (b), each one characterized by the characteristic impedance of Eq. (2), as

$$Z_f = \frac{1}{n_f}\sqrt{\frac{\mu_0}{\varepsilon_0}}, \quad Z_s = \frac{1}{n_s}\sqrt{\frac{\mu_0}{\varepsilon_0}} \tag{18}$$

and by an electrical length $\theta_{f,s} = \beta_{f,s} l$ [4] where $\beta_{f,s}$ is the propagation constant of the fundamental mode and of the second harmonic mode which are solutions of equation (9), and $l$ is the longitudinal length in which the effective index is constant. At the dielectric interfaces of the step discontinuities are placed the current $I_{f,s}$, and the voltages generators $V_{f,s}$ as in the dielectric multilayered waveguides [4] in order to provide a convergent solution. As example of simulation we consider an asymmetric waveguide (see Fig. 1 a)) with a grating on the GaAs core: the total grating length is $L = 5\Lambda$ with $\Lambda = 6.021$ $\mu$m (quasiphase matching QPM condition [6]), d = 0.22 $\mu$m, D = 0.36 $\mu$m, $\chi^{(2)}$(GaAs) = 200 pm/V, $n_1$(GaAs) = 3.374, $n_2 = 3.1$, $n_3 = 1$. By applying the effective dielectric constant EDC approach [5] the calculated effective refractive indices are $n_{f1} = 3.1052$, $n_{s1} = 3.2313$, $n_{f2} = 3.1895$, $n_{s2} = 3.3187$. In Fig. 2 are reported the time evolution of the fundamental mode ($\lambda = 1.55$ $\mu$m) and of the SH mode ($\lambda = 0.775$ $\mu$m) in the slab

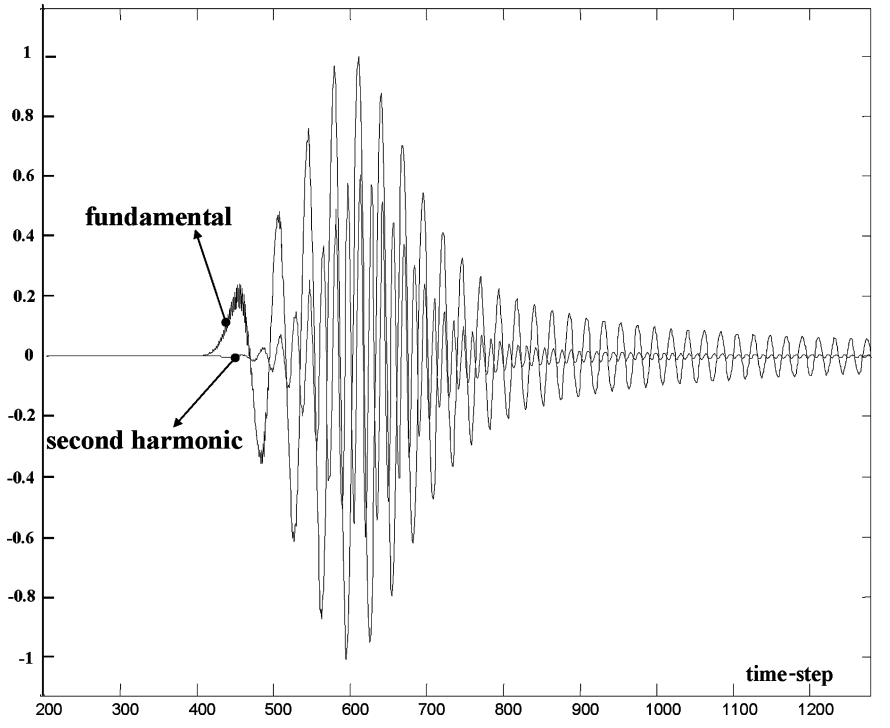


**Figure 2.** Time evolution: normalised amplitude of the fundamental and second harmonic mode.

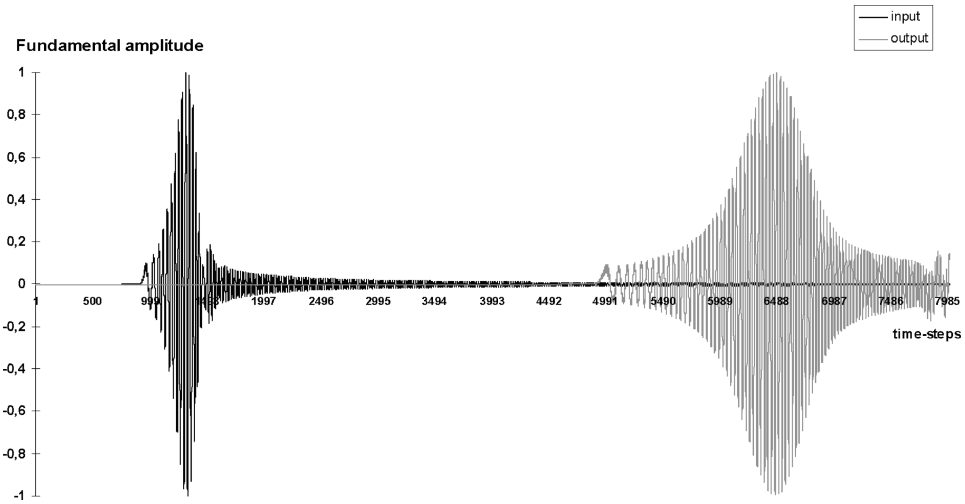


**Figure 3.** Time evolution of the fundamental mode amplitude at input and at output of the grating region.

waveguide before the grating region, considering as source a carrier $V_g$ (with working wavelength of $\lambda_0 = 1.55\ \mu$m) modulated by an exponential signal. Figure 3 and Fig. 4 show the time evolution of the fundamental and the SH normalized signals at the input and at the output of the grating region, respectively. The discrete Fourier transform (DFT) of the fundamental and of the SH signal at different cross sections of the grating (see Fig. 5) validates the presence of the coupled SH signal obtained by the solution of the coupled equations (5) and (6).

The circuit modeling describing the discontinuous optical slab waveguide can be applied also to cavities which can characterize a spontaneous parametric down conversion

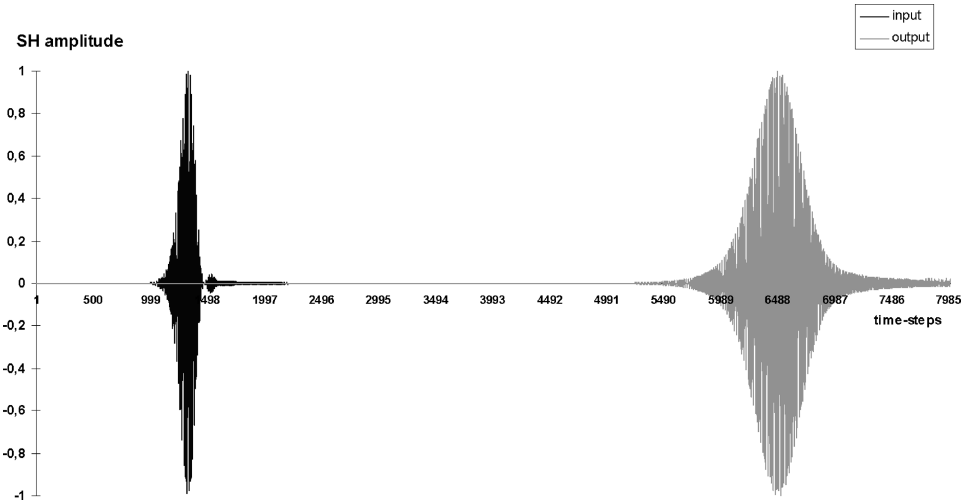


**Figure 4.** Time evolution of the second harmonic amplitude at input and at output of the grating region.

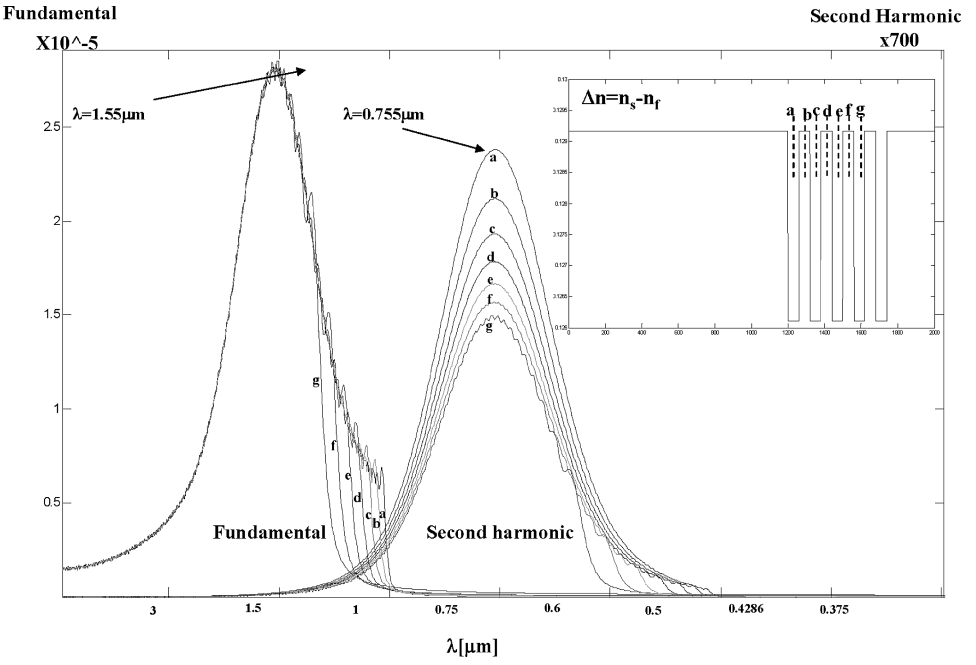


**Figure 5.** Spectra of the fundamental and of the second harmonic mode for different grating cross section. Inset: grating cross sections.

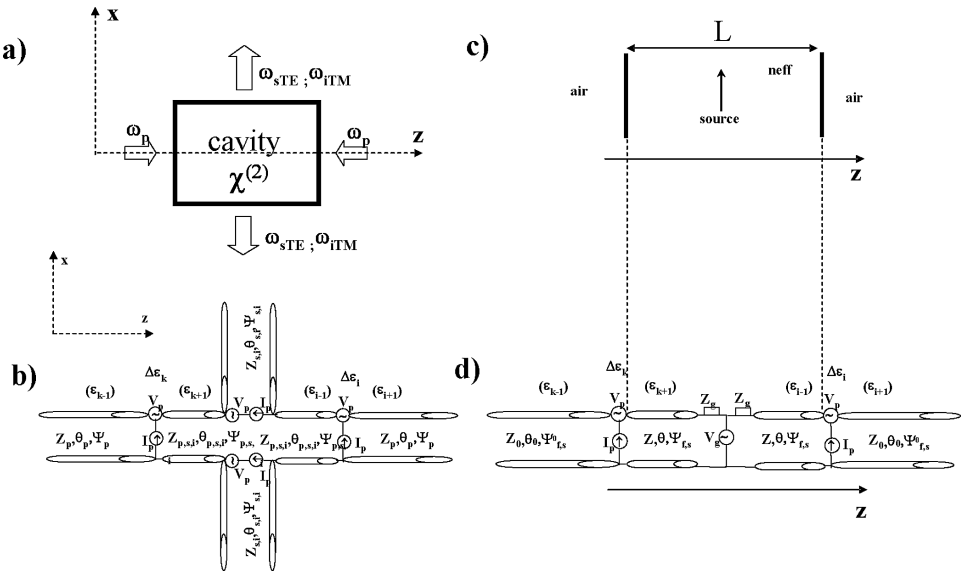


**Figure 6.** a) Signals in twin photon generation process with cavity, and b) related transmission line modelling with generators. c) Monodimensional cavity and d) related transmission line modelling with generators.

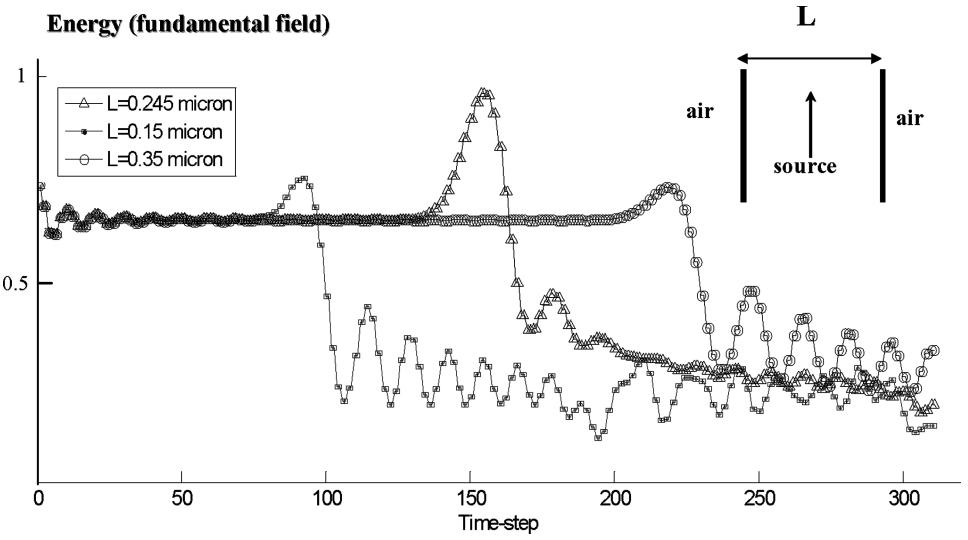


**Figure 7.** Fundamental field: energy stored in the cavity for different lengths L.

process. The coupled equations (2), (3) and (4) for a generic three-wave-mixing process can refer also to a twin photon generation process [7]. In this case a pump signal $\Psi_e$ at pump angular frequency $\omega_1 = \omega_{\rm p}$, a transverse electric (TE) polarized signal $\Psi_h$ at angular frequency $\omega_2 = \omega_{\rm sTE}$, and a transverse magnetic (TM) polarized idler signal $\Psi_g$ at $\omega_3 = \omega_{\rm iTM}$, describe the spontaneous parametric down conversion process. The pump signal excites the nonlinear cavity along the z-direction by generating, in the transverse x-direction (see Fig. 6a)), upward and downward photon pair characterized by energy conservation $\nabla\omega_{\rm p} = \nabla\omega_{\rm sTE} + \nabla\omega_{\rm iTM}$. The signal and the idler fields generated in the cavity propagate as TE/TM modes along the orthogonal x-direction [7]. We validate the cavity

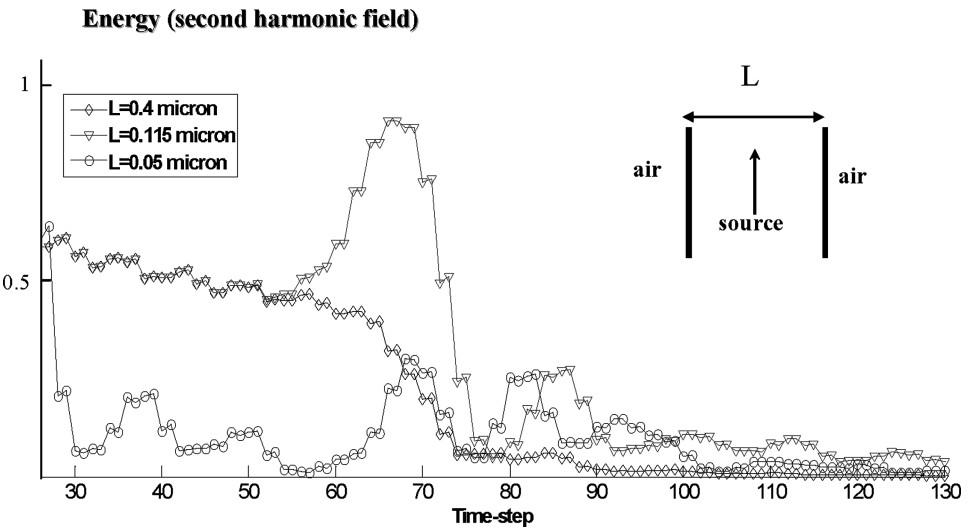


**Figure 8.** Second harmonic field: energy stored in the cavity for different lengths L.

modeling of a SH process by considering a GaAs nonlinear cavity in air (see Fig. 6b)). It is possible to verify the resonances of the fundamental $\Psi^f$ and of the SH $\Psi^s$ field by evaluating the energy stored in the cavity for different cavity lengths. The energy stored in the cavity is calculated as:

$$\int_L (\Psi^{f,s}(z;t))^2 \mathrm{d}z \tag{19}$$

where $L$ is the cavity length. In Fig. 7 and Fig. 8 the energies of the fields are shown for different lengths $L$. In particular, as expected, the maximum peak energy stored is found for $\mathrm{L} = (1.55\ \mu\mathrm{m}/2)/\mathrm{n}_f = 0.245\ \mu\mathrm{m}$ in the case of the fundamental field, and for $\mathrm{L} = (0.755\ \mu\mathrm{m}/2)/\mathrm{n}_s = 0.115\ \mu\mathrm{m}$, in the case of the generated SH signal.

## 3. Conclusion

A flexible and computationally efficient circuital applied to the second-order nonlinear processes of asymmetric slab waveguides and cavities, is presented. The scalar potential modelling is successfully applied to nonlinear optical waveguides with dielectric interfaces. With the help of the EDC approximation the scalar potential method can be generalized to complex 3D optical devices.

## References

1. T. Rozzi and M. Farina, *Advanced electromagnetic analysis of passive and active planar structures*. London: IEE Electromagnetic wave series 46; 1999.
2. C. G. Someda, *Onde elettromagnetiche*. Torino: UTET Ed.; 1996.
3. M. A. Alsunaidi, H. M. Masoudi, and J. M. Arnold, A time-domain for the analysis of second harmonic generation in nonlinear optical structures. *IEEE Photon. Technol. Lett.* **12**, 395–397 (2000).
4. A. Massaro and T. Rozzi, Rigorous time-domain analysis of dielectric optical waveguides using Hertzian potentials formulation. *Opt. Express* **14**, 2027–2036 (2006).
5. A. Massaro, M. Grande, R. Cingolani, A. Passaseo, and M. De Vittorio, Design and modeling of tapered waveguide for photonic crystal slab by using time-domain Hertzian potentials formulation. *Opt. Express* **15**, 16484–16489 (2007).
6. E. U. Rafailov, P. L. Alvarez, C. T. A. Brown, W. Sibbett, R. M. De la Rue, P. Millar, D. A. Yanson, J. S. Roberts, and P. A. Houston, Second-harmonic generation from a first-order quasi-phase-matched GaAs/AlGaAs waveguide crystal. *Opt. Letters* **26**, 1984–1986 (2001).
7. L. Striscione, M. Centini, C. Sibilia, and M. Bertolotti, Entangled guided photon generation in (1+1)-dimensional photonic crystals. *Phys. Rev. A* **74**, (2006).